# A point process approach to analyze spatial transformation effects on threshold exceedances

Madrid, Ana Esther
*Department of Statistics and O.R., University of Granada*
*Campus Fuentenueva s/n*
*Granada E-18071, Spain*
*anaesther@ugr.es*

Angulo, José Miguel
*Department of Statistics and O.R., University of Granada*
*Campus Fuentenueva s/n*
*Granada E-18071, Spain*
*jmangulo@ugr.es*

Mateu, Jorge
*Department of Mathematics, University Jaume I of Castellon*
*Campus Riu Sec*
*E-12071 Castellon, Spain*
*mateu@mat.uji.es*

Risk indicators used in the context of spatial and spatio-temporal analysis are commonly related to the structure of excursion sets defined by threshold exceedances. In Madrid, Angulo and Mateu (2011), marked point process techniques are applied to study pattern-related characteristics of such sets depending on the underlying process properties such as local variability and dependence ranges. In a previous paper, Angulo and Madrid (2010) analyze the effect of deformation and blurring transformations on geometrical-probabilistic characteristics of spatial and spatio-temporal threshold exceedance sets under different scenarios. These types of transformations are meaningful both from physical and methodological points of view in a broad variety of fields of application. In this work, based on simulated realizations from a flexible model family, both approaches are combined in the study of structural changes in excursion sets -viewed as a collection of spatially distributed isolated critical events defined by connected components- derived from deformation and blurring transformations. Specifically, features such as aggregation/inhibition distribution patterns, as well as local anisotropy, are investigated in relation to the local contraction/dilation effects of deformation, and smoothing properties of blurring.

## Introduction

Risk indicators used in applications are usually formulated in relation to the possibility of occurrence of extremal events defined by exceedances over critical thresholds. Structural characteristics of threshold exceedance sets as, for example, recurrence and persistence, are intrinsically related to the properties of the generating model. These properties can be modified by transformations such as deformation and blurring, meaningful for a variety of problems and applications. Deformation can be used as an approach to define flexible classes of non-homogeneous random fields from homogeneous ones (among others, see Sampsom and Guttorp 1992; Anderes and Stein 2008; and the references therein) or in warping techniques as a mean to approximate heterogeneously behaved processes in terms of simpler homogeneous models (see, for example, Glasbey and Mardia 1998, 2001; Mardia et al. 2006). On the other hand, the blurring is a smoothing operator which has been used, in the spatio-temporal context, to represent the diffusive transmission of information between different times

(see Brown et al. 2000).

In Angulo and Madrid (2010), the effect of such types of transformations of threshold exceedance sets on the geometrical characteristics, namely the Euler characteristic and hypervolume, is studied in relation to fractality and long range dependence parameters, as well as on the threshold specifications. These geometrical characteristics have special interest to define risk indicators since, under suitable conditions, the Euler characteristic can be used to approximate the probability of having at least one point in a critical state, whilst by means of the hypervolume it is possible to compute the probability that a generic point of the domain exceeds the threshold (see Adler and Taylor, 2007).

Given the fragmented nature of the excursion sets, a complementary analysis based on marked point process techniques to examine structural heterogeneities is considered in Madrid, Angulo and Mateu (2011). There, heterogeneities in size variations and spatial distribution (clustering/inhibition) patterns of connected components, as well as certain characteristics related to local anisotropy are investigated again depending on underlying specific characteristics.

Here we combine both approaches to analyze how the local contraction/dilation properties of deformation, and smoothing effect of blurring change the characteristics of point patterns defined by the connected components in the transformed threshold exceedance sets, under different scenarios regarding the properties of underlying model and the threshold specifications.

**Methodology and simulations**

Let X be a spatial random field on $D \subset \mathbb{R}^2$. Let $\Phi : D \to D' \subset \mathbb{R}^2$ be a spatial deformation, such that $\Phi$ is a $C^1$-diffeomorphism with positive Jacobian, $|J_\Phi| > 0$. The deformed random field $X[\Phi]$ is defined by

$$X[\Phi](\boldsymbol{s}) = X(\Phi^{-1}(\boldsymbol{s})), \quad \forall \boldsymbol{s} \in D'$$

Now we assume that the random field $X$ is defined on the whole space $\mathbb{R}^2$, and let $h : \mathbb{R}^2 \times \mathbb{R}^2 \to \mathbb{R}$ be a kernel such that $h \geq 0$ and $\int_{\mathbb{R}^2} h(\boldsymbol{s}, \boldsymbol{s}')d\boldsymbol{s}' = 1, \quad \forall \boldsymbol{s} \in \mathbb{R}^2$. The blurred random field $X[h]$ is formulated as

$$X[h](\boldsymbol{s}) = h * X(\boldsymbol{s}) = \int_{\mathbb{R}^2} h(\boldsymbol{s}, \boldsymbol{s}')X(\boldsymbol{s}')d\boldsymbol{s}'$$

In this paper we consider simulated realizations on the square $[-400, 400]^2$ of Cauchy random fields defined by the homogeneous and isotropic covariance function $C(r) = \sigma_X^2(1 + r^\alpha)^{-\beta/\alpha}$, $\alpha \in (0, 2]$ and $\beta > 0$. The parameter $\alpha$ determines the fractal dimension, $D = n + 1 - \alpha/2$ (for a random field on $\mathbb{R}^n$), and independently, for $\beta \in (0, 1)$ the process has long memory with Hurst coefficient $H = 1 - \beta/2$ (see Gneiting and Schlather, 2004). In addition, we define two spatial deformations, $\Phi_1$ and $\Phi_2$, in terms of landmark-based thin-plate splines, to have different contraction and dilation properties, particularly at the central area of the squared domain considered. Specifically, in each of both cases, sixteen landmark points are considered, sharing a subset of eight boundary anchor points (that is, points forced to remain fixed under the deformation), consisting of the four corners and the four edge middle points, to prevent significant distortion of the square borderlines. For $\Phi_1$, the eight interior points $(0, -200)$, $(0, 200)$, $(-200, 0)$, $(200, 0)$, $(-100, -100)$, $(100, 100)$, $(-100, 100)$, and $(100, -100)$ are forced to move half distance towards the square central point, i.e. the origin (0,0); that is, they are respectively transformed into the points $(0, -100)$, $(0, 100)$, $(-100, 0)$, $(100, 0)$, $(-50, -50)$, $(50, 50)$, $(-50, 50)$, $(50, -50)$. On the other hand, $\Phi_2$ is based on the reciprocal assignments. For the blurring a Gaussian kernel $h$ with variance $\sigma_h^2 = 0.5$ has been used.

A point process is a stochastic model governing the locations of events $\{x_i\}$ in some set $D$, where $D$ is considered a bounded region in $\mathbb{R}^2$ (Stoyan et al. 1995). If locations contain associated measurements or marks, the point process is referred to as a marked point process. Considering a fixed

threshold, we can build a spatial point pattern through the centroids of the connected components defining the excursion sets. Associating the size and orientation as marks, marked point processes are defined. To illustrate the effect of the two spatial deformations and the blurring kernel previously defined, Figure 1 displays the excursion sets based on simulated realizations of $X$ in plot (a), $X[h]$ in plot (b) and $X[\Phi_1]$ and $X[\Phi_2]$ in plots (c) and (d) respectively, for the threshold corresponding to the 95th percentile of the simulated realization of $X$ and considering $\sigma^2_X = 0.1$, $\alpha = 2$, and $\beta = 0.1$.

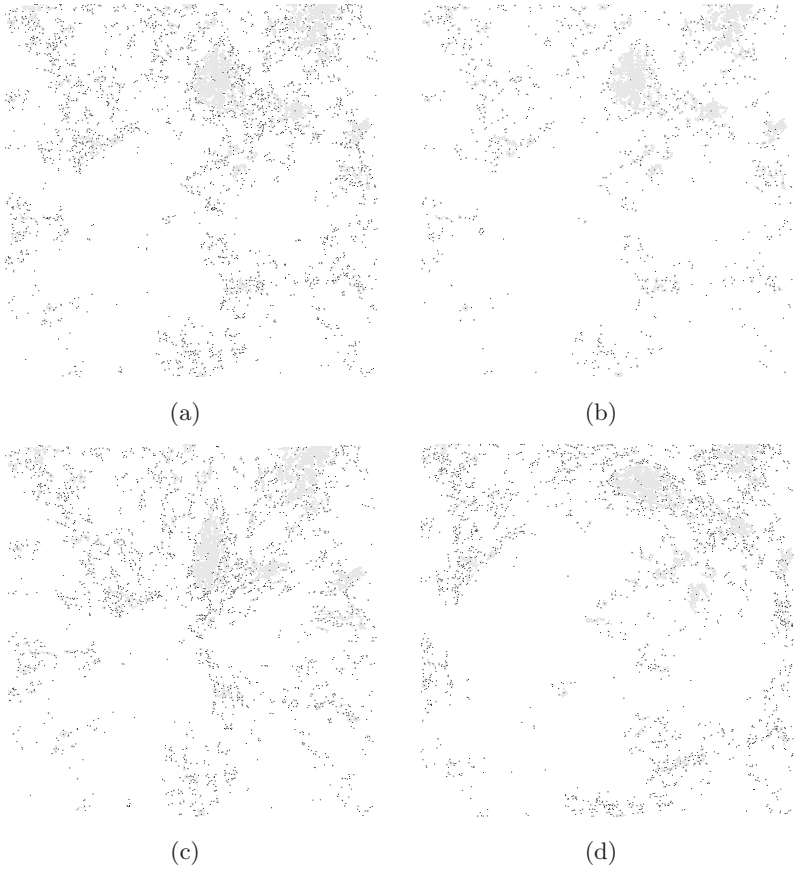


***Figure 1: Excursion sets for the threshold corresponding to percentile 95th of the original realization based on simulated realizations of: (a)*** $X$***; (b)*** $X[h]$***; (c)*** $X[\Phi_1]$***; (d)*** $X[\Phi_2]$***. Black dots represent centroids of connected components.***

The behaviour of both deformations, $\Phi_1$ and $\Phi_2$, varies within the domain and with the local properties of contraction or dilation. Thus, hereafter we just focus on the central subregion $[-100, 100]^2$ where deformations $\Phi_1$ and $\Phi_2$ show properties of contraction and dilation, respectively.

In this work, thresholds are defined based on the empirical distribution functions of the original simulated realizations. It must be noted that, in relation to blurring, since it affects the scale of variation of random field, different results would be obtained if thresholds would be determined from the empirical distribution functions of the transformed realizations.

Tables 1 and 2 contain the mean number and size, respectively, of connected components for different crossed combinations of parameter values and specifications of the threshold computed from 15 simulated realizations of the random field $X$, $X[\Phi_1]$, $X[\Phi_2]$ and $X[h]$. In the deformation case, the increase/decrease of the number of connected components (number of extreme events) is directly related to the way the area of the region is affected by contraction or dilation. However, the smoothing effect due to blurring produces both a decrease in the disaggregation rate of the threshold exceedance sets, and in the variation range, which depends on the local characteristics of the random field.

| 90th percentile of X | | | | |
|---|---|---|---|---|
| | $X$ | $X[\Phi_1]$ | $X[\Phi_2]$ | $X[h]$ |
| $\alpha = 0.5$, $\beta = 0.1$ | 737.71 | 789.28 | 195.26 | 158.13 |
| $\alpha = 2$, $\beta = 0.9$ | 743.33 | 1130.9 | 187.26 | 238.4 |

| 95th Percentile of X | | | | |
|---|---|---|---|---|
| | $X$ | $X[\Phi_1]$ | $X[\Phi_2]$ | $X[h]$ |
| $\alpha = 0.5$, $\beta = 0.1$ | 549.06 | 601.71 | 141.93 | 91.93 |
| $\alpha = 2$, $\beta = 0.9$ | 541.13 | 791.93 | 135.06 | 136.8 |

| 97th percentile of X | | | | |
|---|---|---|---|---|
| | $X$ | $X[\Phi_1]$ | $X[\Phi_2]$ | $X[h]$ |
| $\alpha = 0.5$, $\beta = 0.1$ | 406.86 | 438.33 | 103.53 | 57.86 |
| $\alpha = 2$, $\beta = 0.9$ | 397.13 | 564.93 | 100.06 | 82.8 |

***Table 1: Mean number of connected components for different crossed combinations of parameter values and threshold specifications***

| 90th percentile of X | | | | |
|---|---|---|---|---|
| | $X$ | $X[\Phi_1]$ | $X[\Phi_2]$ | $X[h]$ |
| $\alpha = 0.5$, $\beta = 0.1$ | 5.27 | 4.77 | 21.40 | 15.79 |
| $\alpha = 2$, $\beta = 0.9$ | 5.37 | 3.29 | 21.71 | 9.85 |

| 95th percentile of X | | | | |
|---|---|---|---|---|
| | $X$ | $X[\Phi_1]$ | $X[\Phi_2]$ | $X[h]$ |
| $\alpha = 0.5$, $\beta = 0.1$ | 3.64 | 3.41 | 14.32 | 10.49 |
| $\alpha = 2$, $\beta = 0.9$ | 3.69 | 2.33 | 14.92 | 6.43 |

| 97th percentile of X | | | | |
|---|---|---|---|---|
| | $X$ | $X[\Phi_1]$ | $X[\Phi_2]$ | $X[h]$ |
| $\alpha = 0.5$, $\beta = 0.1$ | 2.94 | 2.81 | 11.56 | 8.01 |
| $\alpha = 2$, $\beta = 0.9$ | 3.01 | 1.97 | 11.91 | 5.17 |

***Table 2: Mean size of connected components for different crossed combinations of parameter values and threshold specifications***

It is important to note that if the threshold is fixed, the number and size of the connected components of the excursion sets based on original simulated realizations are similar for the two models considered in Tables 1 and 2. However, they are clearly different when based on blurred realizations.

To study the effect of transformations considered on the distribution patterns we have computed the mean inhomogeneous $L$-functions for different point processes based on 15 realizations. In Figure 2 we represent the mean $L$-functions of the original and transformed point patterns for the 90th and 97th percentiles corresponding to the model with parameter values $\alpha = 2$ and $\beta = 0.1$. The most significant differences regarding the influence of the threshold specifications are observed in the cases of dilation and blurring.

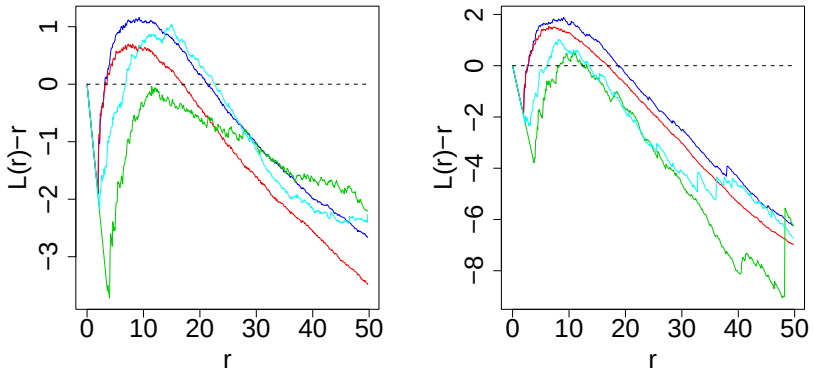


***Figure 2:*** *$L(r) - r$* ***function for the point processes defined by centroids of connected components, for the excursion sets corresponding to threshold associated to percentile 90th (left) and 97th (right) based on the realizations of*** *$X$* ***(blue),*** *$X[\Phi_1]$* ***(red),*** *$X[\Phi_2]$* ***(green), and*** *$X[h]$* ***(light blue).***

## Acknowledgments

This paper has been partially supported by projects MTM2009-13250 and MTM2010-14961 of the SGPI, and P08-FQM-03834 of the Andalusian CICE, Spain.

## REFERENCES

Adler RJ, Taylor JE (2007) *Random Fields and Geometry*. Springer, New York.

Anderes EB, Stein ML (2008) Estimating deformations of isotropic Gaussian random fields on the plane. *The Annals of Statistics* **36**, 719-741.

Angulo JM, Madrid AE (2010) Structural analysis of spatio-temporal threshold exceedances. *Environmetrics* **21**, 415-438.

Brown PE, Karesen KF, Roberts GO, Tonellato S (2000) Blur-generated non-separable space-time models. *Journal of the Royal Statistical Society, Series B* **62**, 847-860.

Glasbey CA, Mardia KV (1998) A review of image warping methods. *Journal of Applied Statistics* **25**, 155-171.

Glasbey CA, Mardia KV (2001) A penalized likelihood approach to image warping. *Journal of the Royal Statistical Society, Series B* **63**, 465-514.

Gneiting T, Schlather M (2004) Stochastic models that separate fractal dimension and the Hurst effect. *SIAM Review* **46**, 269-282.

Madrid AE, Angulo J, Maetu J (2011) Spatial threshold exceedance analysis through marked point processes. *Environmetrics*, submitted.

Mardia KV, Angulo JM, Goitía A (2006) Synthesis of image deformation strategies. *Image and Vision Computing* **23**, 35-47.

Mateu J (2000) Second-order characteristics of spatial marked processes with applications. *Nonlinear Analysis: Real World Applications* **1**, 145-162.

Sampson PD, Guttorp P (1992) Nonparametric estimation of nonstationary spatial covariance structure. *Jour-*

*nal of the American Statistical Association* **87**, 108-119.

Stoyan D, Kendall WS, Mecke J (1995) *Stochastic Geometry and its Applications.* Wiley, New York.